

Nozzle flow control using cavity at supersonic Mach number $M = 1.8$

Abstract

This study investigates the regulation of base flows in a duct with a sudden expansion at a supersonic Mach number. This study utilizes internal flow to simulate the flow area in the recirculation zone within a cavity. This work covers geometrical parameters, including an area ratio of 2.25 and an L/D ratio varying from 1 to 6. To control the base pressure, cavities with w/h ratios of 3:1 and 6:1, and the location of the cavities, were varied from $L/D = 0.5$ to 2. The inertia parameters considered are the expansion levels and Mach number $M = 1.8$. The cavity is employed as a flow control to regulate the base pressure and, consequently, the base drag. Based on the results, it is possible to improve the aerodynamic design to meet the design specifications. This work also provides the design process for a passive control in terms of the cavity for abruptly expanded flow in a nozzle with a supersonic flow Mach number design criteria. The cavity does not negatively affect the nature of the stream.

Keywords: passive control, base flow, Mach number, design Mach number, L/D ratio

Volume 9 Issue 4 - 2025

Muhammad Alif Bin Muhammad Fauzi and
 Sher Afghan Khan

International Islamic University Malaysia, Kuala Lumpur, Malaysia

Correspondence: Sher Afghan Khan, Department of
 Mechanical and Aerospace Engineering, Faculty of Engineering,
 International Islamic University Malaysia, Kuala Lumpur, Malaysia

Received: October 08, 2025 | **Published:** October 21, 2025

Introduction

Base flow shows a decisive role in establishing the vehicle's performance. As an aircraft reaches supersonic speeds, the flow of air around its base can generate significant drag and instability. Therefore, one of the primary issues with aerodynamic vehicles is reducing drag. The force that challenges the comparative movement of a solid moving over a fluid is known as aerodynamic drag.¹ Furthermore, the shear sheet can separate the flow into two center regions. The viscous layer will create powerful vortices, rising the total drag. The total drag force is composed of friction drag, wave drag, and the base drag. As a consequence, base pressure impacts base drag. Because these variables are inversely connected, when base pressure decreases, base drag increases, and vice versa.

Efforts to control or modify the problem can involve both active and passive control methods. Active control strategies typically involve the use of actuators, such as thrusters or control surfaces, to actively manipulate the flow. Passive control, on the other hand, refers to the use of carefully designed shapes, materials, and surface features to influence the behavior of the base flow and mitigate its adverse effects without additional energy input.

At Mach 1.8, the base flow control becomes particularly challenging due to the complex shock wave structures and interactions between the vehicle's surface and the surrounding airflow. Efficiently controlling the base flow at supersonic speeds requires careful design and optimization of the vehicle's shape, surfaces, and aerodynamic features. Researchers and engineers in the aerospace field employ various control methods, such as the use of cavities and ribs, to manipulate shock wave positions, redirect the flow, and reduce turbulence.

Literature review

The literature related to controlling base flows is discussed. The flow at Mach 1.8 is categorized as supersonic, as the Mach number exceeds one. Shock waves are a distinctive characteristic of supersonic streams, triggering brisk changes in flow parameters and streamlines. While the Mach number is more than one, viscous drag, wave drag, and base drag are present. Only base drag is considered in this analysis, and wave drag is negligible.

Furthermore, changing base pressure locations and passive control geometrical aspects influence base drag. Dynamic and inactive flow control strategies can thus be employed to manage the flow. The base pressure was found to be substantially affected by the NPR at the nozzle exit, the passage area ratio, and the diameter of the enlarged duct. This study centers on the operation of passive flow control.

External flow versus internal flow

Two methods of fluid flow studies will be discussed: External flow and internal flow. To begin, the external flow refers to the boundless flow that permeates across bodies. Figure 1 illustrates the sudden increases in external flow.

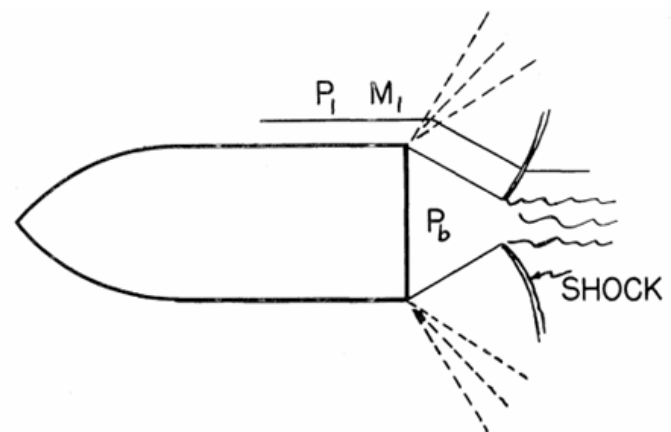
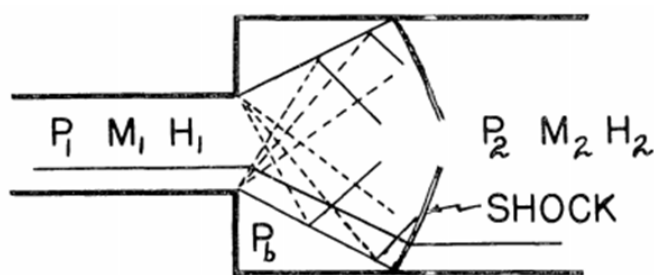


Figure 1 External sudden expansion flow.²

Internal flows, on the contrary, are defined by flowing media surrounded by solid media. Wick,² describes two flow present possibilities where internal flow occurs past an abrupt rise in area in a compressible fluid. The author stated that the flow will initially affect the arduous. The flow will be wedged by the entry when the Mach number, M , is one or greater. When the entering flow Mach is less than unity, however, the flow is altered by the flow beyond the inlet. Second, as the author stated, when the flow Mach number at the inlet is unity or greater, the force at the corner is established by incoming flow specifications. Figure 2 demonstrates the abrupt increase in internal flow.

Figure 2 Internal sudden expansion flow.²

Wick,² further emphasized the alterations and resemblances between the two classes of flow previously mentioned. There are three distinctions between internal and external flows. First, only in internal flow do wall shear forces act on the recirculation region and reattached shear layer. Second, the pressure slopes of equivalent wall segments will vary due to the interior flow of the abrupt expansion. Third, the jet boundary and the expansion waves will connect at weak lines, with the Mach waves beginning to face the inner flow corner. However, there is one similarity between the two streams: the presence of a wake region in each.

Passive control

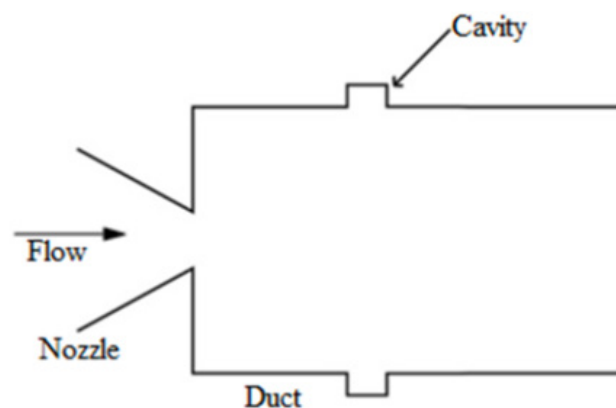
A device's airflow can be managed using either a passive or active control mechanism. The systems are used to control the flow through the device, including the Mach number and flow pressure. When no external energy is necessary to control the flow, the system is said to be passive. In other words, the drag in the flow field is controlled by making geometrical modifications to the flow field. Although active systems are far more successful than passive systems when adaptability is necessary, Moutinho et al. (2010) believe that, in terms of dependability, cost, and maintenance, the passive control method should be the first choice. That is due to passive control, which produces the necessary output without the need for a separate mechanism, such as a weight increase, which can affect a body's aerodynamics. A flow control mechanism can be achieved by altering the appearance and segments of the expedient & increasing supplementary structural elements to it. "Every reasoning that dominates or hinders vortex coming off in 2-D flows usually tends to a rise in base pressure and a subsequent decline in base drag."³ The purpose of any implementation remains the same: to boost base pressure while decreasing base drag. Several passive controls are actively being researched to manage the base pressure. They include cavities, ribs, splitter plates, a locking vortex mechanism, and other features.

Cavities

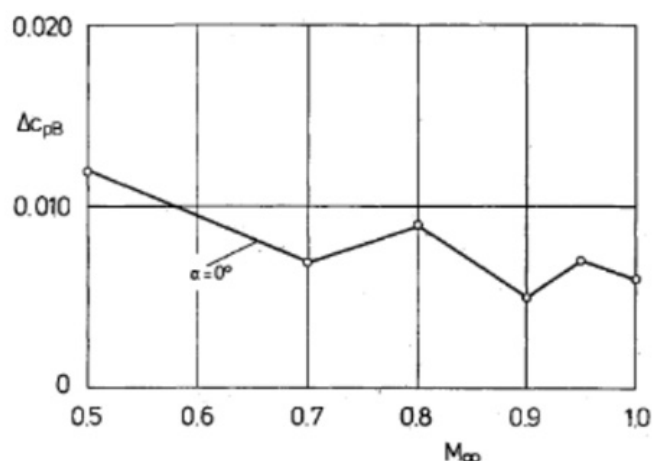
Many cavities are classified as active, passive, reactive, continuous, or discontinuous. Due to the intricate details of cavern flow, it is essential to understand the methods used within and outside of it, as well as their impact on base pressure, which necessitates a comprehensive approach.⁴ In his study, two counter-rotating eddies within the cavities are confined; this approach intends to produce a favorable pressure gradient. The confined vortices over the sucking shallow will establish a distinct sub-atmospheric pressure area, developing with less drag. Owing to the cavities, the lift-to-drag ratio is enhanced.

Tanner,⁵ created a study base cavity with angles of attack ranging from zero to twenty-five degrees. The wind-tunnel tests produced consequences for a base cavity at angles of attack affected by extension faces on base pressure. Figure 3 displays the cavity's base

pressure coefficient, Δc_{pB} , at Mach numbers, M_∞ , ranging from 0.5 to 1.0 at an angle of incidence of 0° .

Figure 3 Cavities in the enlarged duct.⁵

The non-dimensional parameter of base pressure in the presence of a cavity base is larger than the base pressure coefficient for the ordinary base without a cavity, as shown in Figure 4. Furthermore, as described by Tanner,⁵ Morel (1979) investigated the influence of base cavity depths and T/D on the base pressure at zero angle of attack. According to the findings, the deeper the base cavity, the greater the decrease in the base pressure. As a result, in axisymmetric flow, a base cavity may dramatically enhance base pressure while declining base drag.

Figure 4 The graph of base pressure coefficient versus Mach number at $\alpha = 0^\circ$.⁵

Ribs

The rib is used when the cavity starts to function as a "closed cavity," resulting in inefficient passive control. The location of the rib helps stop the flow from rejoining with the shear layer in the base zone. The ribs, as opposed to cavities, are projections, and the secondary vortex created by these projections is expected to produce desirable base pressure values and an enhanced wall pressure distribution.

Sethuraman et al. further suggest that maintaining an optimal height is critical to preventing the ribs from behaving as forward-facing steps.

This behavior causes a secondary vortex to form in the flow, weakening the primary vortex and generating back pressure, which in turn raises the base pressure. The pressure decrease within the zone must be limited to increase the drag.

Islam (2018) discovered the optimal shape of a rib in his research. The article explains how several rib angles and shapes were used to determine the best rib shape. The flow through several types of ribs is simulated using CFD software. As a result, in Islam's (2018) study, the pressure drop for the isosceles triangle is the lowest. As such, it demonstrates that it is the best option.

According to Ranjan et al. (2016), the isosceles right triangle rib will result in an extra energy deficit. This energy will increase the mean friction element due to the laminar sublayer, lowering the Reynolds number. According to Ranjan et al., a secondary flow will be formed around the apex of the triangle. This flow interacts with the main flow, which affects flow reattachment and recirculation between the ribs (Figure 5).

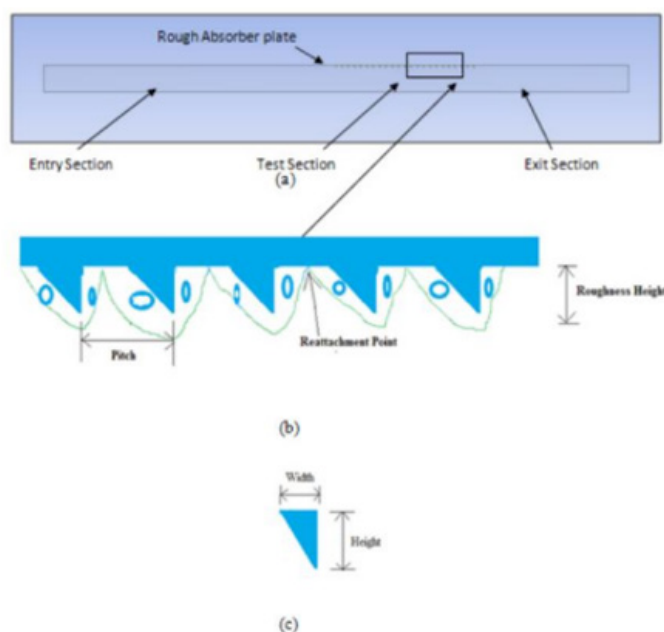


Figure 5 Isosceles triangle rib.

Based on Rathakrishnan's⁶ findings, the numerical ANSYS Fluent code is first validated to obtain and comprehend the correct physics of flow inside the duct, given unexpectedly increased flows with a single rib at various locations. He employed five ribs in a 25-mm-diameter circular duct with aspect ratios of 3:1, 3:2, and 3:3 at a 1D position. Based on his experiments, he found that the 3:1 ratio is the greatest successful in minimizing base drag (Figure 6).

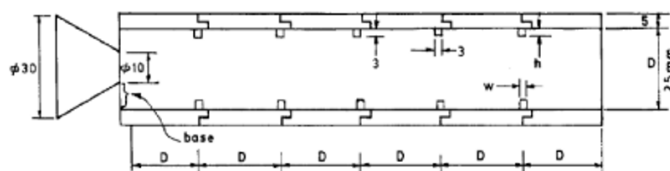


Figure 6 The duct with five ribs in Rathakrishnan's experiment.

Khan et al.⁴ also performed a numerical simulation to evaluate the stream at Mach unity with a pipe diameter of 20 mm. At various positions (1D to 4D), a single rib with three unique aspect ratios (3:1, 3:2, and 3:3) is located one at a time alongside the perimeter of the duct. As a result, when there is no rib case, the NPR increases from 1.5 to 5, and the base pressure reduces. The NPR is the regulating variable used to provide $M < 1$ and $M = 1$ flow settings at the nozzle exit for favorable and perfect expanded conditions. As the Mach

number increases from a small value, the subsonic Mach ultimately reaches a Mach number of unity. The base pressure in the rib case, on the other hand, continuously decreases with an aspect ratio of 3:1. In contrast, it increases with aspect ratios of 3:2 and 3:3 at NPRs of 2.5 & 2, correspondingly. It is observed that the base pressure in the absence of control decreases continuously. In contrast, the base pressure for the ribbed case (3:1) decreases continuously, remaining higher than for the other two rib dimensions.

A reverse flow about the base from the reattachment point area within the boundary layer of an under-expanded sonic flow. The duct must be long enough for the stream to rejoin and the viscous layer to expand. As a result, the duct's L/D ratio is the determining element in reattachment and the enlargement of the shear layer in the bigger duct. Vijayaraja et al. (2014) propose a minimum L/D ratio of 4, and if the L/D number is less than this, the flow may not reconnect at all.

The previous discussion assumed the existence of ribs as a flow control method in expanding ducts without ribs. While ribs are placed in the expanded duct until NPR 3, the base pressure has not varied much. That could result from the increasing flow reconnecting with the downstream wall. A rib downstream of the base region and inverse flow from the boundary layer, which spreads after the reattachment point, interrupts the entire process. When a rib is placed upriver of the wall connecting point, the reversal flow in the recirculation zone changes, but the suction-generating vortex remains unchanged. Therefore, because the ribs may act as fences to prevent reversal flow, the base pressure with ribs will differ from that without ribs. As a result of the presence of ribs in the duct, there is greater suction at the base.

The spot of the rib in the expanded duct is claimed to have a substantial impact on the pressure fluctuations. This assertion has not been extensively tested, and there is no evidence to support the correctness of the method employed to explain the implications of ribs on fluctuations. In limited experiments, ribs were proven more useful as jet 20 control components than cavities. Previously, researchers mainly focused on ribs for specific Mach values and rib positions. As a result, the full potential of this control strategy remains undiscovered.

Concluding remarks

Based on the preceding discussions, passive control appears to be the most practical method of adjusting the base flow at Mach 1.8, without requiring external energy and without adding additional weight to the body, which could result in another aerodynamic effect. The simplistic design of all passive controls makes them easy to construct and requires minimal production expense. Passive control is a modification made to the blunt body to improve base pressure and, ultimately, decrease base drag, resulting in efficient vehicle performance with reduced fuel consumption. Two types of passive control were discussed in this report: cavity and rib. The cavity is an excellent passive control, as its dimensions and positions can be adjusted in various ways. Many studies have been conducted on cavities, and the key functional idea is to produce a resulting vortex that collides with the original vortex, thereby enhancing the base pressure and decreasing drag. When the cavity starts to act like a barred cavity, another control device, the rib, is proposed.

Methodology

Throughout this chapter, the main topic of discussion will be the research method. The section begins with a flowchart, which then proceeds through the convergent-divergent nozzle. Next, the development of the CFD simulation was described, starting with the

design of the geometry, mesh generation, and the establishment of boundary conditions. This section concludes with a check for mesh independence, in which the right mesh size is decided. This study will aid in comprehending how the geometries of the model affect the base pressure and how to regulate it (Figure 7).

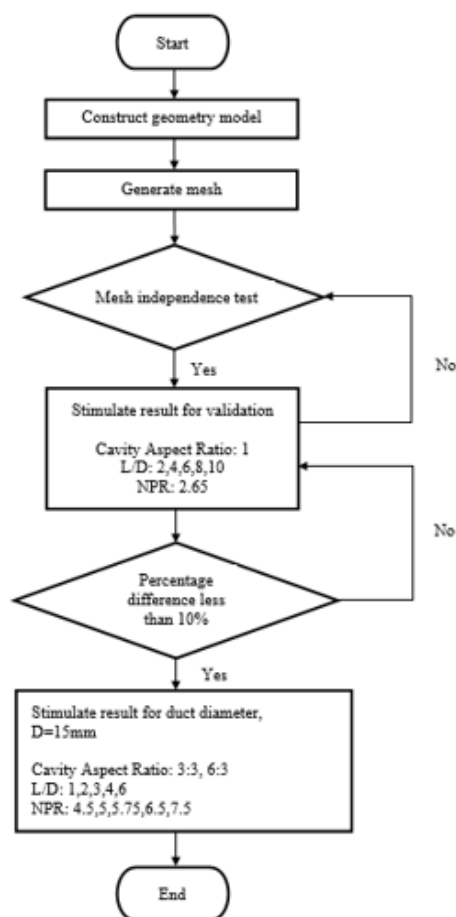


Figure 7 Flow chart.

Convergent-divergent nozzle

A convergent-divergent nozzle is meant to achieve supersonic flow. (Figure 8) depicts the entire dimension of the convergent-divergent nozzle. When dealing with high-speed flow, a diverging duct is used to increase velocity, while a converging duct is used to reduce velocity. The Mach number, area, and velocity are abbreviated as M , A , and u , respectively, for the convergent and divergent regions of the duct.

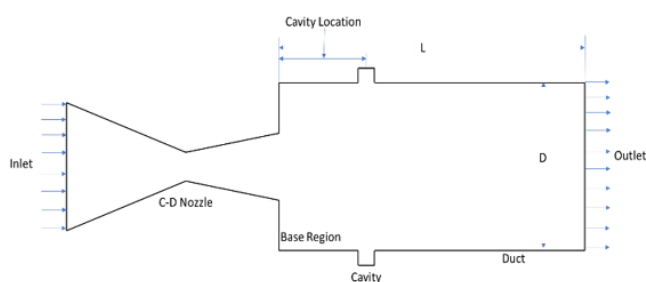


Figure 8 CD nozzle – duct assembly with the cavity.

Computational fluid dynamics (CFD) execution

Computational Fluid Dynamics is an area of fluid dynamics that employs numerical schemes and algorithms to resolve and estimate fluid flow-related challenges. A thorough understanding of computational fluid dynamics includes three essential components: pre-processor, solver, and post-processor.

The creation of geometry

In this project, ANSYS software was utilized to develop the geometry for the model using the Fluent system and Modeler for the geometry creation. (Figure 8) displays an axisymmetric CD nozzle model coupled to a duct with annulated rectangular cavities.

Mesh generation

As the nozzle is axisymmetric, we can use a 2-D case. Based on the assumption that the flow is compressible, the density-based solver was evaluated for this model. That is due to the compressibility of the flow.

The energy equivalence was chosen for the model since the flow is compressible and includes heat transfer. The third hypothesis is that the flow is regarded as turbulent. Accordingly, the k-epsilon (two-equation) model was selected. The k-epsilon model was decided to be Realistic.

An ideal gas was assumed to be a fluid for these materials. The viscosity was resolved to Sutherland's law based on the fourth assumption that the fluid's stickiness is dependent on temperature. Density, specific heat, and thermal conductivity persisted unaffected.

Results and discussion

The first section of this chapter demonstrates the validation of the suddenly expanded CD nozzle as a circular tube, using the control previously carried out by Pandey & Rathakrishnan.⁷ The experiments were conducted at Mach 1.74 and a pressure ratio of 2.65. The selected geometry validations are L/D 2, 4, 6, 8, and 10. Next, the present research is simulated working with the identical model, but with altered geometries to represent Mach 1.8 and various NPRs. The selected NPRs are 4.5, 5, 5.75, 6.5, and 7.5, and the L/D ratios are 1, 2, 3, 4, and 6. The base pressure and contours will be discussed more later in this chapter (Table 1).

Table 1 Present work comparison with previous work and percentage error

L/D	Pandey & Rathakrishnan, 2006	Present work - Ansys fluent		Percentage error (%)
	Base pressure ratio	Pressure (Pa)	Base pressure ratio	
2	0.727	-23753.8	0.766	5.31
4	0.538	-46178.9	0.544	1.16
6	0.523	-51986.1	0.487	6.9
8	0.539	-51143.5	0.495	8.12
10	0.558	-50234	0.504	9.64

The proportion of inaccuracy, evaluated to be less than ten percent, falls within an acceptable range, thereby affirming the validity of the current work. Moreover, (Figure 9) depicts data curves from both the present and previous studies, showing a consistent trend with minimal border fault between data ends. Thus, the validation process is deemed positive.

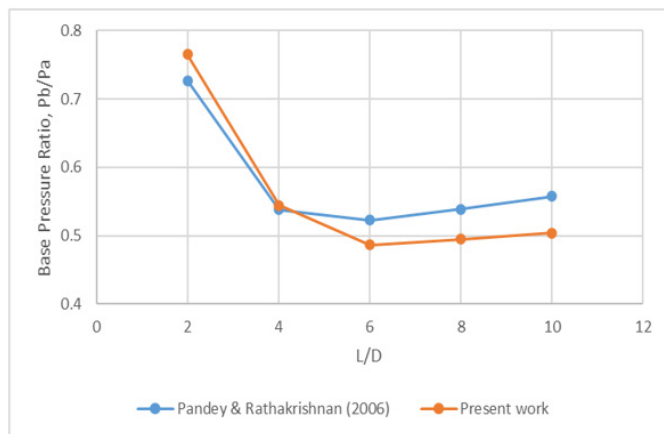


Figure 9 Present study validation

Present work

(Table 2) According to Appendix B,⁸ the NPR for Mach 1.8 is 5.75. The model's design condition served as the established value. In instances of overexpansion, the chosen values were less than the design condition; conversely, for under-expanded scenarios, the selected values exceeded the design condition. (Table 3) outlines the NPRs chosen for the simulation.

Table 2 Present work dimensions

Parameter	Value
Mach number	1.8
Area ratio	2
Convergent angle	20 degrees
Divergent angle	5 degrees
Inlet diameter	25.9 mm
Outlet diameter	10 mm
Throat diameter	8.34 mm
Convergent length	24.12 mm
Divergent length	9.49 mm
Duct diameter	15 mm
Duct length	Depends on L/D ratio

Table 3 Selected NPR

Expansion of a Mach 1.8 nozzle	Nozzle pressure ratio
Over-expanded	4.5, 5
Correctly-expanded	5.75
Under-expanded	6.5, 7.5

The effect of cavity & geometry regarding base pressure

Figure 10 shows the base pressure variations with nozzle pressure ratio at various (L/D) ratios. The cavity appears to be effective at the NPRs required for correct expansion. As long as the jets were over-expanded, control seems to be ineffective. Hence, these results restate that whether the flow control employed is dynamic or inert becomes successful once the stream from the nozzle is either perfectly expanded or under expanded.

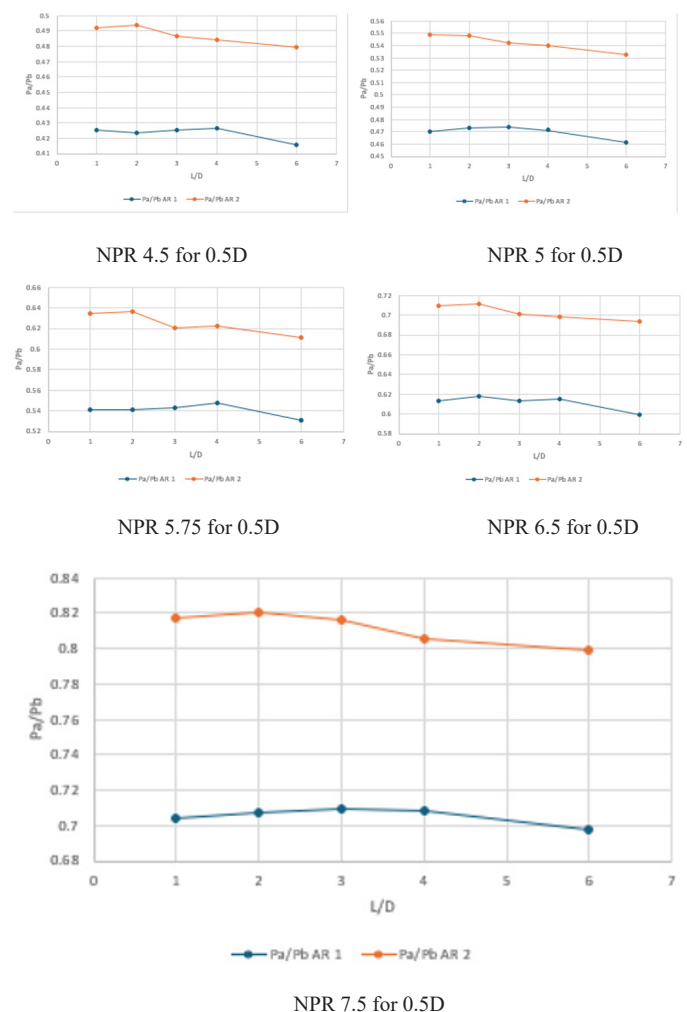
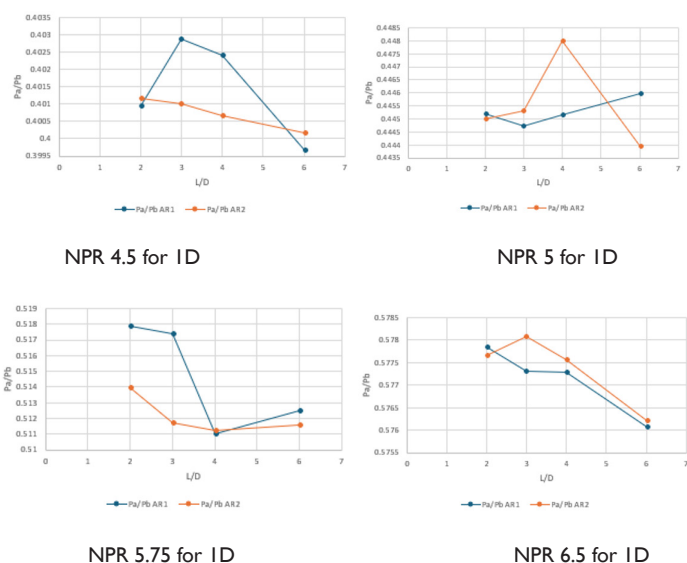


Figure 10 Base pressure alternative L/D at various NPR.

Figure 11 shows the outcomes of base pressure variations for various NPRs, dependent on the L/D ratio. For this case, the lowest duct segment needed appears to be L/D = 2.



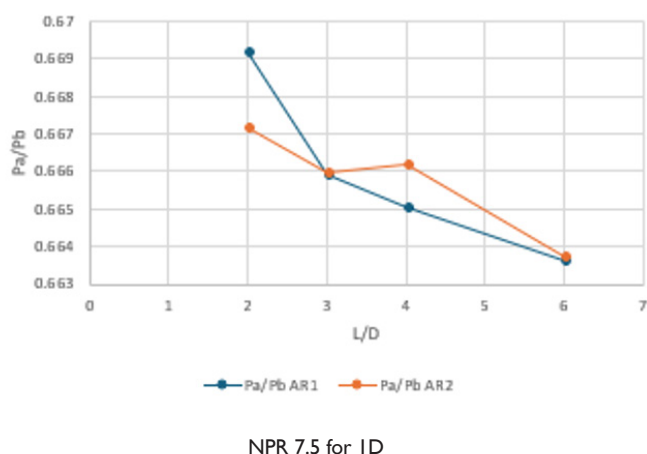


Figure 11 Base pressure variation L/D at various NPR for cavity placed at $L/D = 1$.

Figure 12 presents the base pressure findings when the cavity is located at $L/D = 1.5$. From the outcomes, it is evident that the control will be effective once the flow enters the cavity; otherwise, the flow will not perceive the cavity's presence, and there will be no variations in the base pressure.

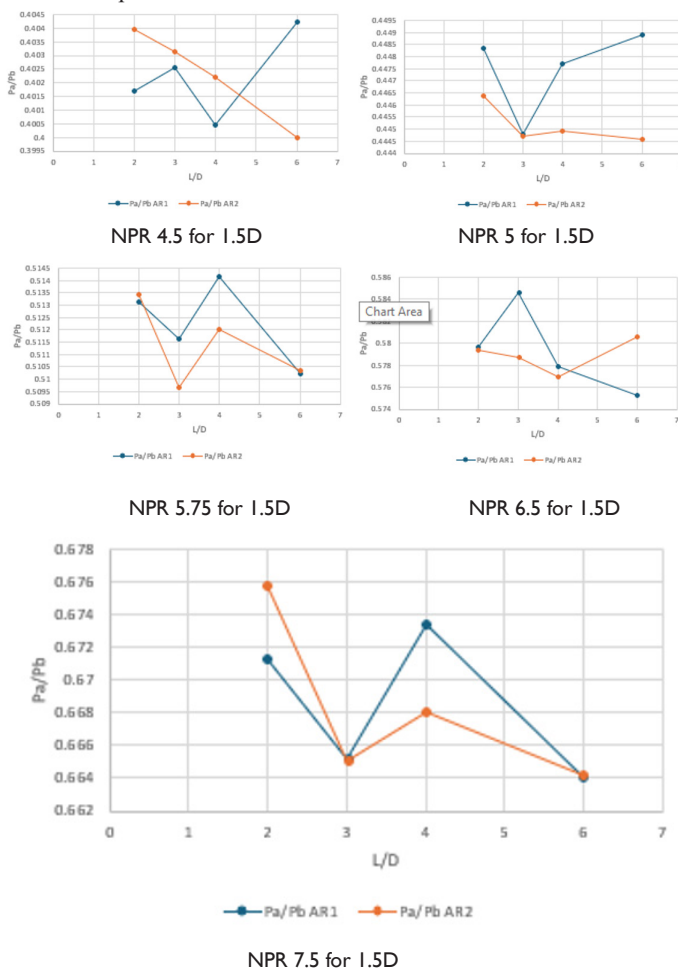


Figure 12 Base pressure alteration L/D at various NPR for cavity located at $L/D = 1.5$.

Figure 13 shows that the cavity is not effective when located at $L/D = 2$.

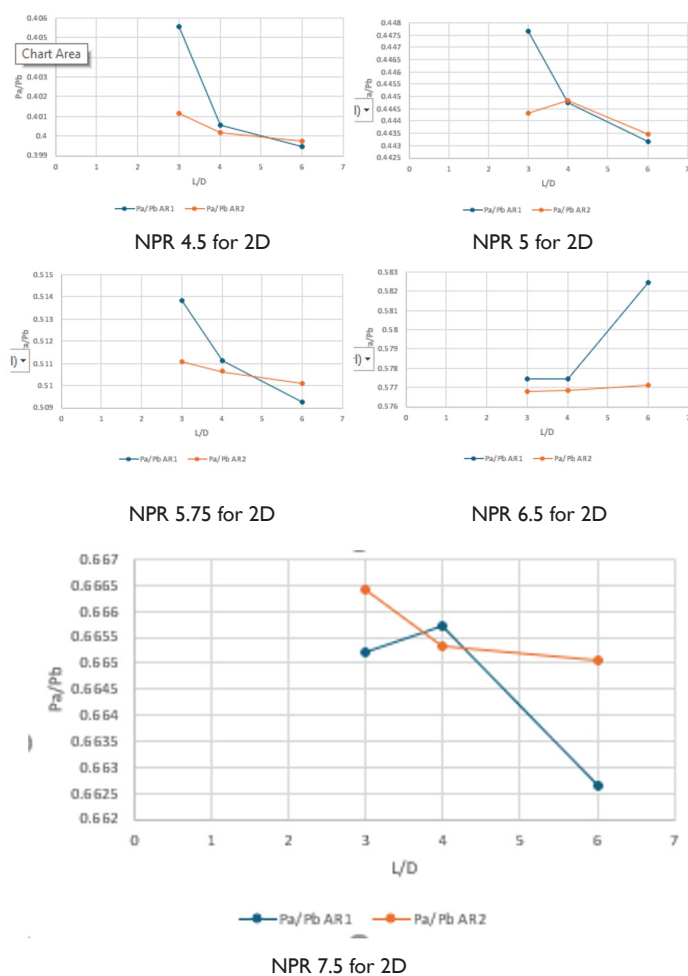
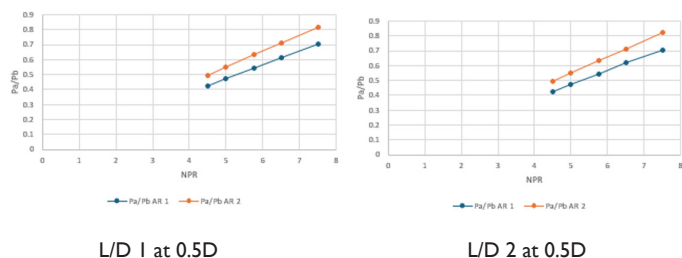


Figure 13 Base pressure variation L/D at various NPR when cavity is placed at $L/D = 2$.

The effect of cavity position from the wall & base pressure

Figure 14 shows the base pressure deviations with levels of expansion for cavity locations at $L/D = 0.5$ for various duct segments. Figure 8 displays the base pressure variations as a function of expansion level for a fixed cavity location at $L/D = 0.5$. From the Figure, it is apparent that the cavity's location allows the flow exiting from the nozzle to fall into it, causing in a significant raise in the base pressure. This linear pattern shows a gradual increase in base pressure with an upsurge in NPR.



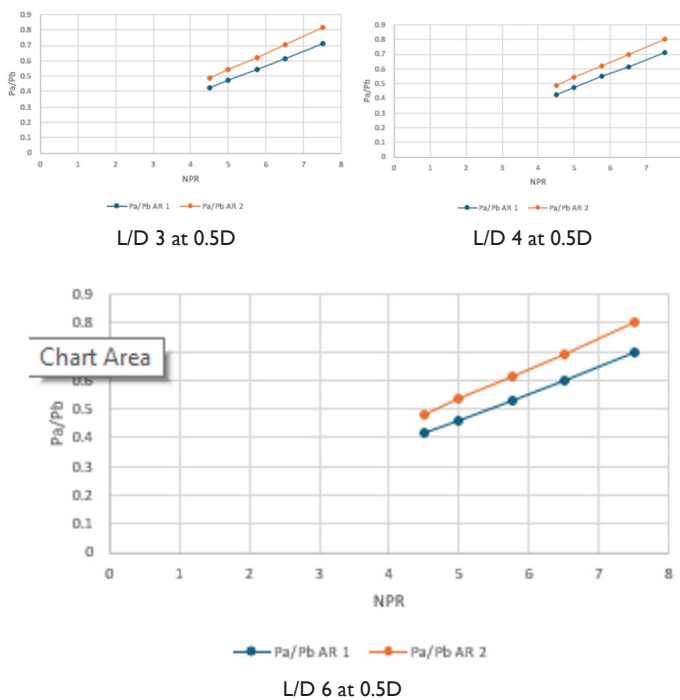


Figure 14 Base pressure alteration NPR for cavity location at $L/D = 0.5$ for various duct lengths.

Figure 15 indicates the variations in the base pressure dependent on NPR when the cavity is located at $L/D = 1$. These results suggest that the presence of a cavity does not influence the base pressure, and the base pressure values with and without control are the same. These results indicate that the cavity becomes ineffective if the dividing streamline does not fall into the cavity.

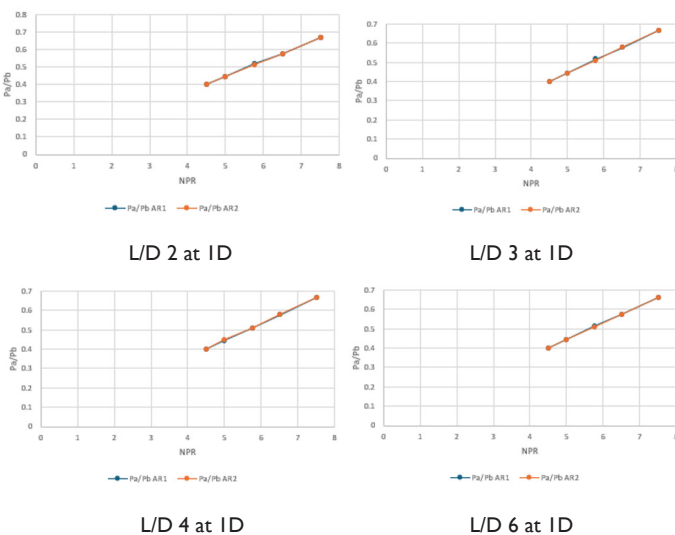


Figure 15 Base pressure variation NPR for cavity location at $L/D = 1.0$ for various duct lengths.

Figure 16 illustrates the variations in base pressure with respect to NPR when the cavity is positioned at $L/D = 1.5$. These results suggest that the presence of a cavity does not influence the base pressure, and the base pressure values with and without control are the same as those observed in the previous case, where the cavity was located at $L/D = 1.0$. These results indicate that the cavity becomes ineffective if the dividing streamline does not fall into the cavity.

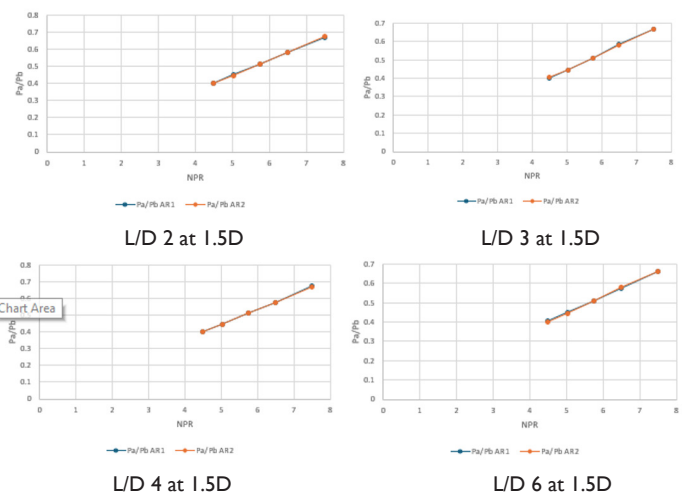


Figure 16 Base pressure deviation NPR for cavity location at $L/D = 1.5$ for various duct lengths.

Figure 17 illustrates the variations in base pressure with NPR when the cavity is located at $L/D = 2.0$. These results suggest that the presence of a cavity does not influence the base pressure, and the base pressure values with and without control are the same as those observed in the previous case, where the cavity was located at $L/D = 1.5$. These results indicate that the cavity becomes ineffective if the dividing streamline does not fall into the cavity.⁹

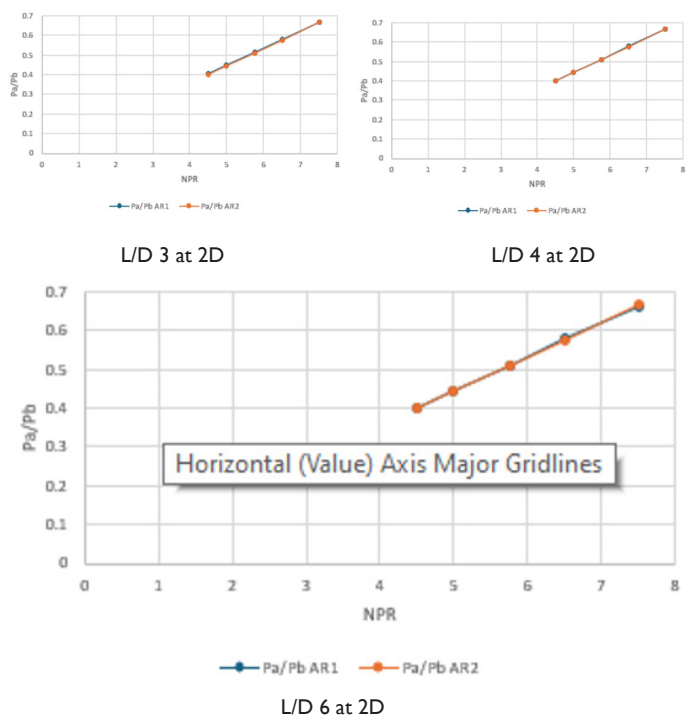


Figure 17 Base pressure variation NPR for cavity location at $L/D = 2.0$ for various duct lengths.

Concluding remarks

In summary, the base pressure is affected by several factors, including the level of expansion, Mach number, area ratio (L/D ratio), cavity dimensions, and cavity position. The effectiveness of passive control is contingent upon the cavity's location, with ineffectiveness noted beyond the reattachment point. Literature review suggests

that both active and passive control measures prove effective when jets experience a favorable pressure gradient, while their efficacy diminishes in over-expanded jet conditions. Interestingly, the depth of the cavity does not significantly impact its effectiveness compared to the length of the cavity. Furthermore, passive control is most effective when the dividing streamline falls within the cavity's length.

For future work, several avenues merit exploration to enhance our understanding of base pressure control and optimize aerodynamic performance in high-speed flows. Further research could explore the development and evaluation of innovative passive control strategies, taking into account emerging technologies and materials. Exploring the influence of real-world conditions, such as turbulence and external disturbances, on the efficacy of passive control methods would also be beneficial.

Furthermore, investigating the application of machine learning algorithms to predict and optimize base pressure under diverse scenarios could open new avenues for efficient aerodynamic design. Collaborative efforts between researchers from fluid dynamics, materials science, and control systems engineering could lead to holistic solutions for base pressure management in high-speed aerodynamic flows.

Acknowledgements

None.

Conflicts of interest

The author declares that there are no conflicts of interest.

Funding

None.

References

1. Gad-el-Hak M. *Flow control: passive, active, and reactive flow management*. Cambridge University Press; 2000.
2. Wick RS. The effect of the boundary layer on sonic flow through an abrupt cross-sectional area change. *J Aeronaut Sci*. 1953;20(10):675–682.
3. Viswanath PR. Passive devices for axisymmetric base drag reduction at transonic speeds. *J Aircraft*. 1988;25(3):258–262.
4. Asadullah M, Khan SA, Soudagar MEM, et al. A comparison of the effect of single and multiple cavities on base flows. *2018 IEEE 5th International Conference on Engineering Technologies and Applied Sciences (ICETAS)*. 2019:1–6.
5. Tanner M. The base cavity at angles of incidence. *AIAAJ*. 1988;26(3):376–377.
6. Rathakrishnan E. Effect of ribs on suddenly expanded flows. *AIAAJ*. 2001;39(7):1402–1404.
7. Pandey KM, Rathakrishnan E. Annular cavities for base flow control. *Int J Turbo Jet Engines*. 2006;23(2):113–127.
8. Oosthuizen PH, Carscallen WE. *Introduction to compressible fluid flow*. 2nd edn. CRC Press; 2014.
9. Tu J, Yeoh GH, Liu C. *Computational fluid dynamics: a practical approach*. Butterworth-Heinemann. 2018.